PERGAMON

Applied Geochemistry 15 (2000) 311–325

Applied Geochemistry

Ba/Sr, Ca/Sr and $^{87}Sr/^{86}Sr$ ratios in soil water and groundwater: implications for relative contributions to stream water discharge

Magnus Land[a,*,1], Johan Ingri[a], Per S. Andersson[b], Björn Öhlander[a]

[a]*Division of Applied Geology, Luleå University of Technology, S-971 87, Luleå, Sweden*
[b]*Laboratory for Isotope Geology, Swedish Museum of Natural History, Box 50007, S-10405, Stockholm, Sweden*

Received 6 April 1998; accepted 21 May 1999
Editorial handling by W.M. Edmunds

Abstract

Barium/Sr and Ca/Sr ratios have been used to model the relative importance of different sources of stream water. Major and trace element concentrations together with $^{87}Sr/^{86}Sr$ ratios were measured in precipitation, soil water, groundwater and stream water in a small (9.4 km^2) catchment in northern Sweden. The study catchment is drained by a first order stream and mainly covered with podzolized Quaternary till of granitic composition. It is underlain by a 1.8 Ga granite. A model with mixing equations used in an iterative mode was developed in order to separate the stream water into 3 subsurface components: soil water, shallow groundwater, and deep groundwater. Contributions from precipitation are thus not included in the model. This source may be significant for the stream water generation, but it does not interfere with the calculations of the relative contributions from the subsurface components. The results show that the deep groundwater constitutes between 5 and 20% of the subsurface water discharge into the stream water. The highest values of the deep groundwater fraction occur during base flow. Soil water dominates during snowmelt seasons, whereas during base flow it is the least important fraction. Soil water accounts for 10–100% of the subsurface water discharge into the stream water. Shallow groundwater accounts for up to 80% of the subsurface water discharge with the lowest values at peak discharge during snowmelt seasons and the highest values during base flow. The validity of the model was tested by comparing the measured $^{87}Sr/^{86}Sr$ ratios in the stream water with the $^{87}Sr/^{86}Sr$ ratios predicted by the model. There was a systematic difference between the measured and modelled $^{87}Sr/^{86}Sr$ ratios which suggests that the fraction of soil water is overestimated by the model, especially during spring flood. As a consequence of this overestimation of soil water the amount of shallow groundwater is probably underestimated during this period. However, it is concluded that the differences between measured and predicted values are relatively small, and that element ratios are potentially effective tracers for different subsurface water flowpaths in catchments.

* Corresponding author. Fax: +1-626-796-9823.
E-mail address: magnus@maxwell.gps.caltech.edu (M. Land).
[1] Present address: Lunatic Asylum of the Charles Arms Laboratory, Division of Geological and Planetary Sciences, California Institute of Technology, Pasadena, CA 91125, USA.

0883-2927/00/$ - see front matter
PII: S0883-2927(99)00054-2

1. Introduction

Despite numerous studies, the origin of stream water is still a matter of controversy. Different runoff mechanisms include both overland flow and subsurface flow (Pearce et al., 1986). According to the classical theory of Horton (1933), overland flow occurs when the intensity of rainfall exceeds the infiltration capacity of the ground. The role of this overland flow in humid areas like Scandinavia has been questioned, since the infiltration capacity is normally larger than the intensity of rainfall or snowmelt (Rodhe, 1981). There are, however, situations during the snowmelt season when the infiltration capacity can temporarily be decreased and Hortonian overland flow may occur, e.g., when ice is present in the soil pores or as layers at the base of the

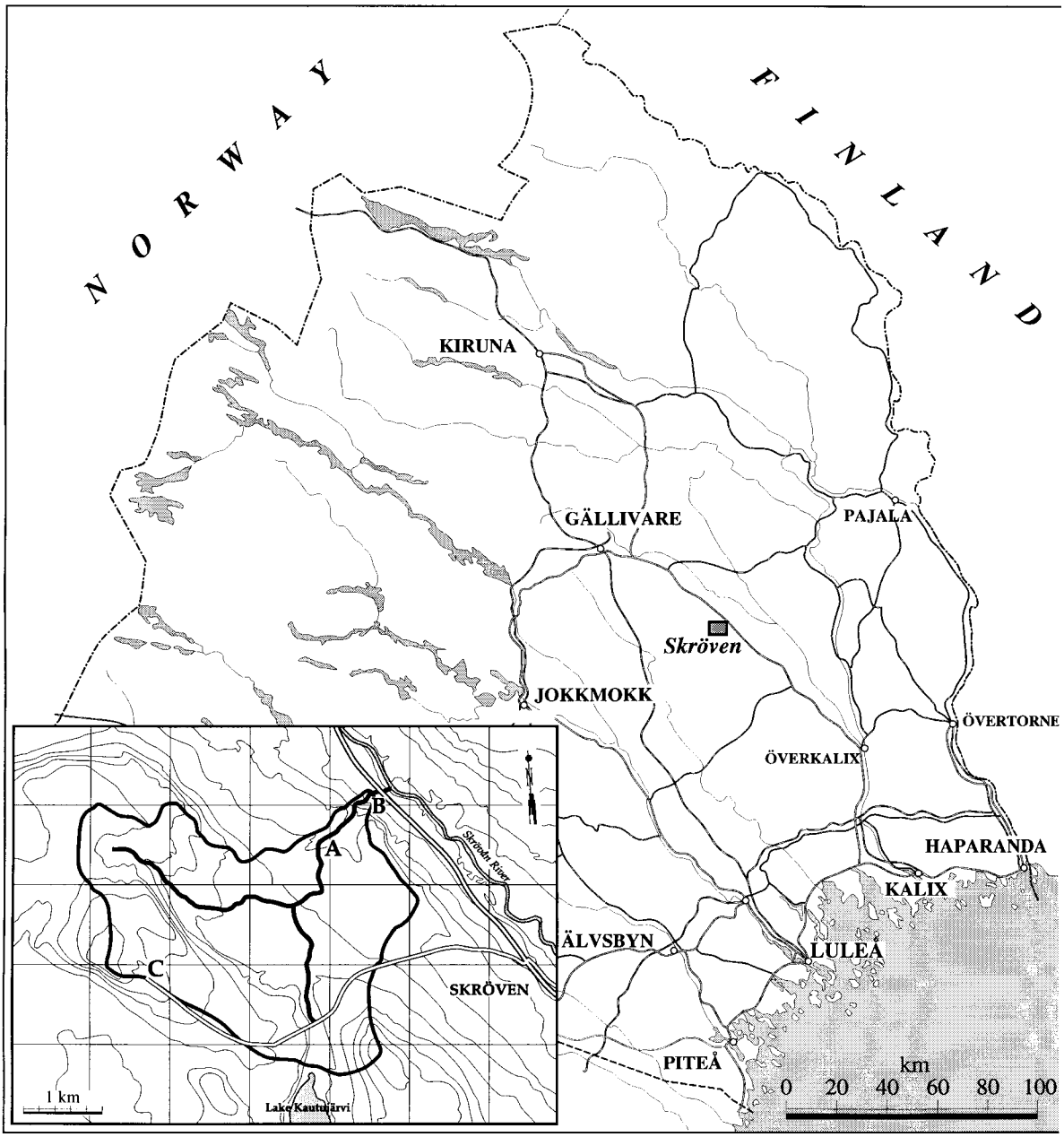

Fig. 1. Map showing the study catchment located at N66°47′ E21°49′. Precipitation, soil water and shallow groundwater was sampled at station A. Deep groundwater and stream water was sampled at stations C and B, respectively.

snow pack (Stein et al., 1994). There may also be saturation overland flow, which consists partly of rainfall on saturated areas, and partly of outflowing groundwater (e.g., Rodhe, 1981). The subsurface flow may be dominated by either rapid throughflow emphasizing macropore flow (e.g., Beven and Germann, 1981; Smettem, 1984; Norrström and Jacks, 1996), or displacement of old water (e.g., Sklash and Farvolden, 1979; Pearce et al., 1986). Stream water during snowmelt or a storm event is often considered a mixture of new water (precipitation) and old water. The old water, or pre-event water, is usually regarded as groundwater. However, recent studies have shown that soil water may also constitute a significant part of the old water component (e.g., Bazemore et al., 1994). In this paper the authors show how Ba/Sr and Ca/Sr ratios can be used to resolve the subsurface flow into different soil water and groundwater components.

Both chemical tracers (e.g., Hooper et al., 1990; Robson and Neal, 1990; Mulder et al., 1991; Wels et al., 1991) and isotopic tracers (e.g., Rodhe, 1981; Maulé and Stein, 1990; Rose, 1996) have been used in various mixing models in order to trace different water masses. If a chemical tracer such as the concentration of an element is used, the relative proportions of the components in a two-component mixture (m) can be calculated according to Eq. (1) (Sklash and Farvolden, 1979; Pearce et al., 1986)

$$X_i = \frac{C_m - C_j}{C_i - C_j} \tag{1}$$

where X denotes relative proportion, i and j denote the components and C is concentration of the tracer element. If element ratios are used as a chemical tracer Eq. (1) cannot be applied, i.e., it is not possible to just substitute the concentrations for the ratios. This is because a component with low concentrations will influence the ratio in a mixture to a lesser extent than a component with high concentrations. Hence, one great advantage of using ratios rather than concentrations is that if a third, very dilute component (e.g., precipitation) is present, it is still possible to calculate a partitioning between two components with high concentrations. Various mixing equations dealing with both isotopic and elemental ratios have been developed (e.g., Langmuir et al., 1978; Li, 1985; Stewart et al., 1998).

In a two component mixture (m), the fraction of the first component (X_i) can be calculated in accordance with Eq. (2) (derived in Appendix A)

$$X_i = \frac{1}{1 - \dfrac{\left(\dfrac{C^a}{C^b}\right)_m C_i^b - C_i^a}{\left(\dfrac{C^a}{C^b}\right)_m C_j^b - C_j^a}} \tag{2}$$

where i and j denote the components, a and b denote the elements, and C is concentration. In this study the authors will use Ba and Ca as element a and Sr as element b.

To validate the use of Ba/Sr and Ca/Sr ratios as tracers, an isotopic tracer has also been employed. In other studies where isotopic tracers have been used in this context, the main focus has been on H and O isotopes. In this study, however, the Sr isotopic composition is used, or the $^{87}Sr/^{86}Sr$ ratio, of the solute Sr. The reason for this choice of isotopic tracer is that the $^{87}Sr/^{86}Sr$ ratio provides information about the sources of Sr (Faure and Powell, 1972), and thus helps to interpret the element/Sr ratios.

2. Sampling area

Samplings were performed in a small catchment (9.4 km^2) situated within the Kalix River watershed (Fig. 1). The catchment is drained by a first-order (second-order during snowmelt) stream which is frozen during winter (December–April). The peak discharge during snowmelt in early May is about 750 l s^{-1}, while the base-flow discharge during summer is 20–30 l s^{-1}. The elevation in the catchment ranges from 110 to 375 m above sea level. The catchment is mainly covered by till with spodosol soil profiles (more than 90% of the area), classified as typic haplocryod according to Keys to Soil Taxonomy (Soil Survey Staff, 1995). Bedrock outcrops and mires add up to less than 7% of the area and there are no lakes in the catchment. The till, supporting mainly pine and spruce forest, is unsorted and consists mainly of granitic material, the principal minerals being quartz, plagioclase (An˜30), K-feldspar and biotite. Thin section studies and X-ray diffraction analysis have shown accessory amounts of amphibole, epidote, zircon, ilmenite, apatite, garnet, and clay minerals (chlorite, smectite and mixed-layer clays). In the B-horizon hydro-goethite ($HFeO_2 \cdot nH_2O$) is also present. It is underlain by a 1.8 Ga granite. The till was deposited approximately 8700 a ago (Lundqvist, 1986). Further details about the soil and weathering profiles in this catchment can be found in Öhlander et al. (1996). Annual precipitation is approximately 560 mm, of which 250 mm evaporates, and the annual mean air temperature is about −0.2°C (SMHI, 1996). The sampling area is relatively uninfluenced by anthropogenic activities.

There is no evidence for the residence time of the groundwater in this particular catchment, but based on ^3H monitoring Eriksson (1974) found that the mean transit time for groundwater in the Råne River watershed in northern Sweden was 3–4 a. The Råne River watershed is similar to, although larger than, the catchment used in this study. It is likely that the mean tran-

sit time for the groundwater in the present study is of the same order of magnitude as it is in the Råne River watershed.

3. Sampling and analytical methods

A bulk composition of the winter precipitation was obtained by sampling snow cores in late April 1994, just before snowmelt. Summer precipitation was collected with a polyethylene funnel (31.5 cm in diameter) connected to a polyethylene container with a silicone tube. The funnel was mounted 2 m above the ground and the container was kept in darkness to minimize biological activity in the collected water. Throughfall was collected in the same way.

Soil water was collected with cylindrical tension lysimeters (length = 95 mm, outer diameter = 21 mm) made of PTFE (polytetrafluoroethene) mixed with glass and with a pore size of 2 μm (Prenart equipment Aps., Fredriksberg, Denmark). Before installation, the PTFE cups and tubings were flushed with 1 l of 1.0 M HCl and then rinsed with 4 l of deionized water. The PTFE cups were installed horizontally from a trench (at least 0.5 m back from the trench face) at 4 depths; at 5 cm in the E-horizon, at 15 cm in the Bs1-horizon, at 40 cm in the Bs2-horizon, and at 100 cm in the C-horizon. A slurry of soil from the installation depths and deionized water was inserted into the holes to ensure good capillary contact between the cups and the soil. The lysimeters were connected to a tensiometer-controlled vacuum pump in such a way that the difference between the vacuum and the soil tension was kept constant (−100 kPa). After installation, the soil water was continuously purged and discarded for 6 weeks prior to any sampling with subsequent analyses. The soil water was then collected twice a month from July to November 1994, and from May to October 1995. However, the sampling was in progress continuously, i.e., each sample contains water sampled for periods of approximately two weeks. In August, no samples could be collected from the E-, Bs1-, and Bs2-horizons due to drought.

Shallow groundwater was sampled from a 5 cm-diameter polyethylene well located in a recharge area (station A, Fig.1). The well (perforated along the lowermost metre) was completed to a depth of 5.2 m, and the depth to the groundwater table in the well varied between 2.3 and 4.6 m below ground surface during one year. The groundwater well was installed in October 1993, and then 5–10 l of groundwater was pumped from the well and discarded approximately every 4 weeks for 6 months. The groundwater was sampled once a week from April to November 1994, and from March to July 1995 with a bailer sampler. On each sampling occasion, one well-volume was discarded before the actual sampling. Land and Öhlander (1997) showed that there can be considerable differences in the chemical composition of shallow groundwater between recharge and discharge areas in this catchment. It was concluded that the differences were caused by mixing with deep groundwater and soil water in discharge areas, whereas the groundwater in the studied recharge area was considered to be representative of shallow groundwater only. The chemical composition of the shallow groundwater in the recharge area did not change significantly during snowmelt or during changing depth to groundwater table. Two deep groundwater samples were collected from a domestic tap water in September 1997 (station C, Fig. 1). The depth of the well is 20–25 m, and the groundwater table is less than 8 m below ground surface at this location. Considering the large distance between stations A and C there is probably not any direct hydraulic contact between these different groundwaters, but it is assumed that they are representative of shallow and deep groundwater, respectively, in this catchment.

Stream water was sampled from April to November 1994, and from May to July 1995 (station B, Fig. 1). The stream water, groundwater and precipitation (including throughfall) were immediately filtered through 0.45 μm Millipore filters in the field and then collected in acid-leached polyethylene containers.

All samples were acidified with suprapure HNO_3 and analysed for major ions and Sr with ICP-AES, and for trace elements (including Ba) with ICP-MS. For Ba, 5 measurements of SLRS-2 deviated $<7\%$ from the certified value, and the precision was better than 8% for all samples (3 replicate analysis). Measurement of SRM 1643c resulted in Ca and Sr concentrations deviating less than 5% from the certified concentrations, and the precision for all samples was better than 5 and 10%, respectively (3 replicates).

The Sr isotopes were analysed with a Finnigan MAT 261 equipped with 5 Faraday cups used in a dynamic mode. Strontium was separated from Rb by a Sr-specific cation-exchange resin (Pin and Bassin, 1992). Approximately 400–1000 ng of Sr were loaded on Re double filaments. Corrections of the obtained data for mass dependent fractionation were made by normalizing to $^{86}Sr/^{88}Sr = 0.1194$. Isobaric interferences from ^{87}Rb were corrected for using ^{85}Rb. The contribution from ^{87}Rb to the measured $^{87}Sr/^{86}Sr$ value was found to be less than 10^{-5}. Total procedural blanks were measured with isotope dilution and were found to be less than 0.1 ng. Measurements of NBS 987 resulted in a mean of 0.710209 ± 0.000028 (2σ) $(n = 24)$.

Table 1
Chemical composition of precipitation and throughfall in the study catchment (Ca–Si in mg l^{-1}, Al–Sr in μg l^{-1})

Element	Snow	Rain	Throughfall
Ca	0.061	< 0.02	0.35
Fe	0.006	0.008	0.03
K	< 0.2	< 0.2	0.53
Mg	< 0.04	< 0.04	0.099
Na	< 0.06	< 0.06	< 0.06
S	0.22	0.37	0.38
Si	< 0.01	0.15[a]	0.61
Al	4.2	8.6	52
Ba	0.53	0.41	4.6
Sr	< 1.0	< 1.0	< 1.0

[a] Probably contamination from the silicone tube used in the sampling device.

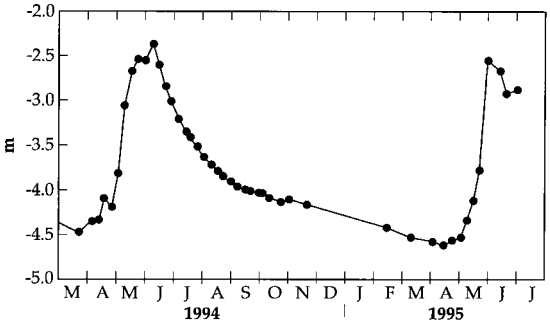

Fig. 2. Depth to groundwater table at the location of shallow groundwater sampling.

4. Results

4.1. Chemical composition of precipitation, soil water, and groundwater

The chemical composition of winter (snow) and summer (rain) precipitation is shown in Table 1. The precipitation in the area is rather dilute, and several elements are present in concentrations well below detection limit. At a monitoring station approximately 45 km south of the study catchment at Skröven, Granat (1990) found the concentrations of Ca, Mg, Na and K to be 0.06, 0.02, 0.11 and 0.08 mg l^{-1}, respectively. These values are precipitation weighted averages for 1990, i.e., both winter and summer concentrations are included. Andersson et al. (1991) measured the Sr concentrations in rainwater at a location approximately 65 km north of the study catchment and derived a median value (P_{50}) of 0.1 μg l^{-1}. The concentration of Sr in throughfall at the same location varied between 3 and 11 μg l^{-1} ($P_{50}=6$ μg l^{-1}, $n = 9$) in pine forest, and between 4 and 20 μg l^{-1} ($P_{50}=6$ μg l^{-1}, $n = 8$) in spruce forest. Snow samples in a transect across central Scandinavia (Andersson et al., 1990) showed that the Sr concentrations decreased with increasing distance from the Atlantic coast, with values ranging from 0.76 to 0.03 μg l^{-1}. It was also found that Sr was more radiogenic farther away from the coast ($^{87}Sr/^{86}Sr$ ratios varied between 0.70976 and 0.71936). Jacks et al. (1989) and Åberg et al. (1989) studied inland localities in central and northern Sweden and found the $^{87}Sr/^{86}Sr$ ratio in snow and rain to be 0.710–0.717 and 0.712–0.719, respectively. Taking these results into consideration, it is assumed for modelling purposes, that the Sr concentration in snow at the location in the present study (320 km from the Atlantic coast) is 0.05 μg l^{-1}, and that the $^{87}Sr/^{86}Sr$ ratio is 0.713. The $^{87}Sr/^{86}Sr$ ratio in rain is assumed to be 0.715. Plants and stemflow usually have the same Sr isotopic composition as soil solution (from which the Sr is derived), while throughfall has a $^{87}Sr/^{86}Sr$ ratio intermediate between rain and stemflow (Nakano et al., 1993). Given that the $^{87}Sr/^{86}Sr$ ratio in soil water is approximately 0.726 (see below), the $^{87}Sr/^{86}Sr$ ratio in throughfall is assumed to be 0.719.

The chemical composition of the soil water is shown as monthly averages in Table 2. During snowmelt in May all elements were diluted by melt water in the E-horizon. After that the concentrations reached a maximum in July for Ba. The highest concentrations of Ca and Sr were reached in October. In the C-horizon the concentrations were fairly constant throughout the study period. It can also be seen that the highest Ba/Sr and Ca/Sr ratios in the E-horizon occur during the summer months, and that the values for the Ba/Sr ratio in the B-horizons are somewhat lower than in the E- and C-horizons. Generally, the highest Ba/Sr and Ca/Sr ratios occur in the E-horizon.

The major part of the groundwater recharge in the study catchment occurred during the snowmelt seasons. These were the only periods during which the groundwater table was elevated, as shown in Fig. 2. The concentrations of major elements and Ba and Sr were fairly constant in the shallow groundwater throughout the study period. The deep groundwater was only sampled on one occasion (September 1997), but there is no reason to believe that the temporal variation should be larger compared to the shallow groundwater. The chemical composition of the groundwater is summarized in Table 3, and the temporal variations in the concentrations of Ba, Ca and Sr in the shallow groundwater are shown in Fig. 4. Table 3 shows that the concentrations of major elements and Sr are higher in the deep groundwater than in the shallow groundwater. For Ba the situation is reversed. Further information about the groundwater in this catchment can be found in Land and Öhlander (1997).

Table 2
Chemical composition of soil water. All numbers are monthly averages. The samples were taken at a depth of 5 cm (E), 15 cm (Bs1), 40 cm (Bs2) and 100 cm (C), respectively

		May	June	July	August	September	October
Ca (mg/l)	E	0.30	1.76	1.89	a	2.84	4.22
	Bs1	0.32	0.24	0.31	a	a	0.76
	Bs2	1.46	1.44	1.15	a	a	
	C	0.67	0.69	0.73	0.70	0.70	0.58
Mg (mg/l)	E	0.086	0.40	0.37	a	0.92	1.1
	Bs1	0.26	0.19	0.19	a	a	0.68
	Bs2	0.46	0.44	0.34	a	a	
	C	0.31	0.38	0.35	0.32	0.34	0.31
Na (mg/l)	E	< 0.06	0.39	0.37	a	1.26	1.28
	Bs1	0.34	0.22	0.19	a	a	0.84
	Bs2	0.081	0.14	0.28	a	a	
	C	0.18	0.50	0.49	0.50	0.64	0.48
K (mg/l)	E	0.54	1.54	1.07	a	2.92	2.66
	Bs1	0.48	< 0.25	0.70	a	a	1.25
	Bs2	< 0.25	< 0.25	< 0.25	a	a	
	C	< 0.25	< 0.25	< 0.34	< 0.33	< 0.25	< 0.25
Si (mg/l)	E	0.35	4.77	5.80	a	9.19	7.66
	Bs1	2.37	3.22	3.96	a	a	5.15
	Bs2	2.56	2.83	2.95	a	a	
	C	2.68	2.88	3.04	3.26	2.96	2.33
Ba (μg/l)	E	2.1	13.5	22.7	a	13.5	18.0
	Bs1	1.9	2.2	3.1	a	a	3.4
	Bs2	3.5	6.4	5.9	a	a	a
	C	5.2	5.9	7.1	6.7	5.9	5.0
Sr (μg/l)	E	2.0	10.0	10.0	a	17.0	24.0
	Bs1	3.0	3.5	4.5	a	a	9.0
	Bs2	11.0	11.5	10.0	a	a	a
	C	6.0	5.5	6.2	6.0	6.0	5.0
Ca/Sr	E	150	175	189	a	168	176
	Bs1	107	68	70	a	a	84
	Bs2	133	125	115	a	a	a
	C	111	125	117	119	116	119
Ba/Sr	E	1.0	1.5	2.3	a	0.81	0.75
	Bs1	0.63	0.65	0.70	a	a	0.38
	Bs2	0.32	0.57	0.59	a	a	a
	C	0.86	1.1	1.2	1.2	0.98	1.0

[a] Not analysed.

4.2. Chemical composition of stream water

The discharge in the stream is shown in Fig. 3. During base flow the discharge is approximately 20 l s^{-1}, while at peak discharge during snowmelt the discharge is higher than 700 l s^{-1}.

The concentrations of all major elements and Sr in the stream water decreased during spring flood, whereafter they increased to the same values as before snowmelt (Fig. 4). There was also a clear decrease in pH and alkalinity during the spring flood. The pH decreased from 7.1 at base flow to approximately 5.5 during spring flood. In contrast to the major elements and Sr, the concentration of Ba increased at the beginning of the spring flood. However, at a later stage of the spring flood Ba was also diluted and remained low throughout the year. During next spring flood the concentration of Ba increased again (Fig. 4).

4.3. $^{87}Sr/^{86}Sr$ ratios

The $^{87}Sr/^{86}Sr$ ratios in soil water, groundwater and stream water are shown in Table 4. Arrows in Fig. 4 indicate which groundwater and stream water samples were analysed for Sr isotopes.

Two soil water samples from the E-horizon and two samples from the C-horizon were analysed for Sr isotopes. The samples from the E-horizon yielded higher

Table 3
Average (x) chemical composition of groundwater and stream water during one year. (Ca–Si in mg l^{-1}, Ba and Sr in μg l^{-1}, and alkalinity in μeq l^{-1}. σ = standard deviation, and n = number of samples)

	Shallow groundwater			Deep groundwater[a]			Stream water[b]		
	x	σ	n	min	max	n	x	σ	n
Ca	2.43	0.12	39	17.1	17.1	2	2.57	0.74	36
Fe	< 0.02	0.01	28	0.016	0.040	2	0.498	0.31	36
K	0.875	0.20	39	2.44	2.49	2	0.475	0.26	24
Mg	0.528	0.04	39	4.80	4.84	2	0.703	0.21	36
Na	1.60	0.28	39	4.51	4.68	2	1.17	0.34	36
S	0.616	0.04	40	1.99	2.09	2	0.653	0.22	36
Si	4.46	0.25	39	7.04	7.09	2	3.39	0.74	36
Alkalinity	208	13.5	20	620	–	1	143	71.5	35
Ba	3.89	0.31	39	2.00	3.05	2	3.75	1.26	36
Sr	21.9	1.3	39	51.3	53.0	2	14.1	3.85	36
Ca/Sr	111	4.6	39	323	333	2	182	9.69	36
Ba/Sr	0.178	0.018	39	0.039	0.058	2	0.288	0.12	36

[a] Due to the limited number of samples only minimum and maximum values are given.
[b] Not flow weighted.

ratios than the samples from the C-horizon at a confidence level of 90% ($p = 0.0581$), but the difference is rather small. There was no significant difference between the samples within the same horizon, although the samples were collected during different hydrological conditions (late snowmelt and base flow, respectively).

The Sr isotopic composition of the shallow groundwater was rather constant throughout the studied period and did not seem to be affected by snowmelt and subsequent recharge. At a confidence level of 99% ($p = 0.0060$), the $^{87}Sr/^{86}Sr$ ratio in the shallow groundwater was higher compared to the ratio in the C-horizon soil water. However, the difference is relatively small. There was no statistically significant ($p = 0.6776$) difference between the $^{87}Sr/^{86}Sr$ ratios in the shallow groundwater and the soil water from the E-horizon. The deep groundwater samples showed values significantly higher than the values in soil water and shallow groundwater.

The $^{87}Sr/^{86}Sr$ ratio in stream water was intermediate between deep and shallow groundwater. There is no obvious seasonal variation of the $^{87}Sr/^{86}Sr$ ratio, but the available data indicate that the ratio was slightly increased during snowmelt. A similar sesonal variation was also observed by Bullen et al. (1997) in two central Sierra Nevada streams.

Table 4
Sr concentrations and $^{87}Sr/^{86}Sr$ ratios in soil water, groundwater, and stream water

Date of sampling	Sample	Concentration (μg l^{-1})	$^{87}Sr/^{86}Sr$	Hydrologic condition
June 1995	Soil water, E-horizon	9.0	0.726533	Late snowmelt
July 1995	Soil water, E-horizon	10	0.726842	Base flow
October 1994	Soil water, C-horizon	6.0	0.724981	Base flow
June 1995	Soil water, C-horizon	6.0	0.725006	Late snowmelt
May 1994	Shallow groundwater	24	0.727121	Peak discharge
September 1994	Shallow groundwater	20	0.726633	Base flow
May 1995	Shallow groundwater	22	0.726457	Early snowmelt
May 1995	Shallow groundwater	21	0.726040	Peak discharge
September 1997	Deep groundwater	53.0	0.760505	Base flow
September 1997	Deep groundwater	51.3	0.760551	Base flow
May 1994	Stream water	6.0	0.738680	Peak discharge
September 1994	Stream water	18	0.738123	Base flow
May 1995	Stream water	22	0.738803	Early snowmelt
May 1995	Stream water	11	0.738577	Mid-snowmelt

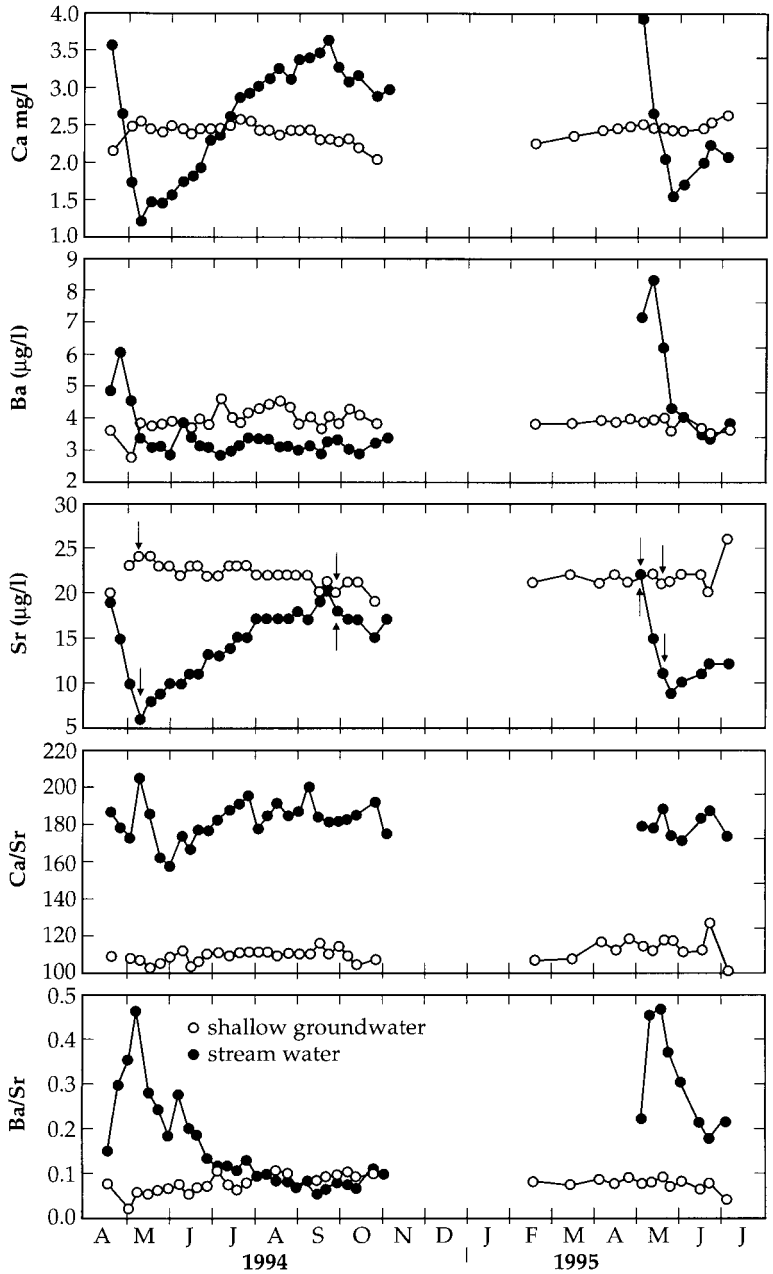

Fig. 4. Seasonal variations in concentrations of Ca, Ba, and Sr, and Ba/Sr and Ca/Sr ratios in shallow groundwater and stream water. The arrows in the Sr-plot indicate samples analysed for Sr isotopes.

5. Discussion

5.1. Ba/Sr and Ca/Sr ratios

Element ratios in water have been used as tracers in earlier works. For example, Négrel et al. (1993) used major and trace element ratios in their study of the Congo basin. Ingri et al. (1997) used S/Mg ratios when evaluating the hydrogeochemistry of S isotopes in the Kalix river catchment, northern Sweden, and Ingri et al. (1998) used major element ratios to trace water from different bed rock areas in the same catchment. The idea behind the use of Ba/Sr and Ca/Sr ratios as tracers is that Ba and Sr occur in different minerals with different weathering susceptibility. In felsic magmas both elements occur in trace amounts and do not

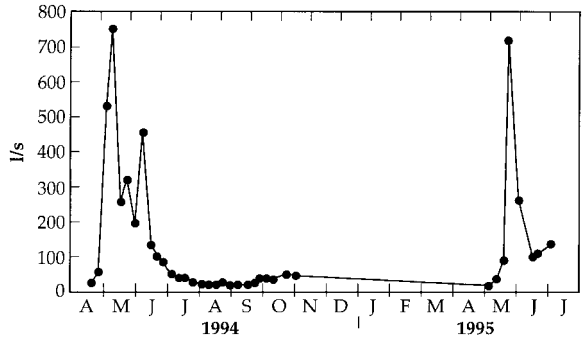

Fig. 3. Seasonal variation in stream water discharge.

form any important minerals of their own (Stueber, 1978; Puchelt, 1972). Usually, Sr substitutes for Ca or K, whereas Ba usually substitutes for K (Mason and Moore, 1982). Generally, the K-minerals in granitoids are more resistant to weathering than the Ca-minerals. The release of Ba to soil solution should therefore demand a more intensive weathering than the release of Sr, and as weathering intensity decreases with soil depth, so should the dissolved Ba/Sr ratio.

Analogous to Ba/Sr the dissolved Ca/Sr ratio may also vary with depth. Two important carriers of Ca and Sr in granitic rocks are plagioclase and amphibole. However, Sr has a much stronger affinity for plagioclase than amphibole (Stueber, 1978). The Ca/Sr ratio in a quartz-feldspar concentrate and an amphibole concentrate from a lithology in northern Sweden comparable to the one at the study catchment are 39.6 and 1037, respectively. If amphibole is less resistant to weathering and has a higher Ca/Sr ratio than feldspar, and weathering intensity decreases with soil depth, the dissolved Ca/Sr ratio should increase with soil depth. As indicated by the relatively high Ba/Sr and Ca/Sr ratios in throughfall (>4.6 and >350, respectively), biological cycling of nutrients may also influence these ratios in the uppermost part of the soil. The biophilic coefficient of Sr (0.06) is smaller than that of Ca (0.17), but close to that of Ba (0.04) (Perel'man, 1977). Also, it cannot be excluded that ion exchange and adsorption may contribute to the observed variations of the Ba/Sr and Ca/Sr ratios. Nesbitt et al. (1980) found in a weathering profile of a granodiorite that Ba was retained on clays to a much larger degree than Ca and Sr. They also observed a preferential exchange onto the clays of Sr relative to Ca. The problems associated with such non-conservative behaviour will be discussed briefly in a later section.

In Fig. 5, Ba/Sr and Ca/Sr ratios are plotted for soil, soil water, groundwater, and stream water. The fact that the dissolved Ba/Sr ratio generally is lower than the ratio in the solid soil indicates that Ba actually occurs in minerals more resistant to weathering compared to the minerals hosting Sr (at least in the E-horizon where the low pH (4.28) makes significant adsorption unlikely). All water samples are undersaturated with respect to $BaSO_4$. Furthermore, the dissolved Ba/Sr ratios in the soil water and groundwater generally show a decreasing trend with depth. The deviation from this trend in the B-horizon (pH 5.5–6.25) might be explained by preferential adsorption of Ba on clays and Fe oxy-hydroxides. It can also be seen from the Ba/Sr ratios that soil water (or throughfall) appears to be an essential component of the stream water.

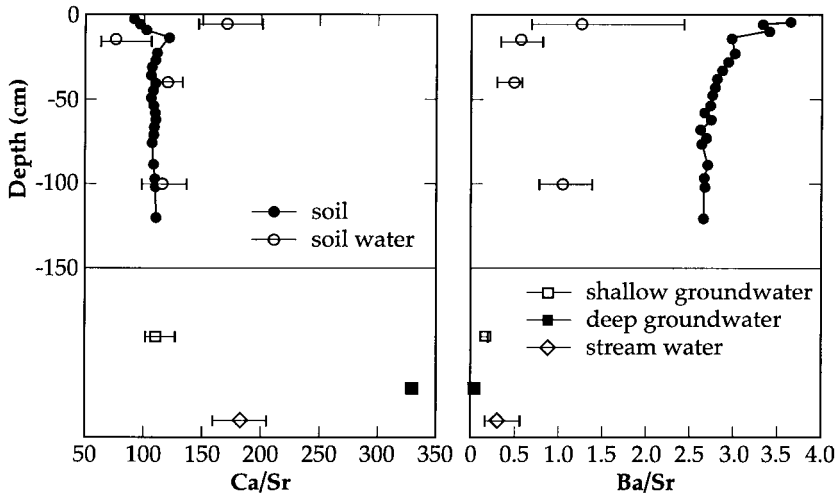

Fig. 5. Ca/Sr and Ba/Sr ratios (average and range) in soil, soil water, shallow groundwater, deep groundwater, and stream water.

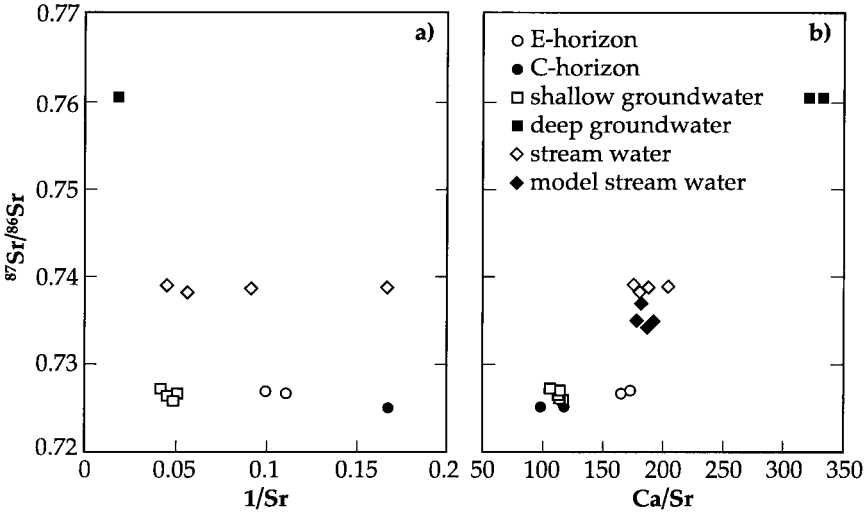

Fig. 6. $^{87}Sr/^{86}Sr$ vs 1/Sr and Ca/Sr for soil water, shallow groundwater, deep groundwater and stream water. The stream water discharge on the stream water sampling occasions was (from left to right) 20, 30, 110 and 750 l s^{-1}, respectively.

The Ca/Sr ratio in the soil water shows a negative correlation with the Ca/Sr ratio in the solid soil. In the soil water the Ca/Sr ratio is highest in the E-horizon and lowest in the B-horizon, whereas in the solid soil the situation is reversed. Preliminary results from selective leaching studies suggest that the enhanced solid Ca/Sr ratio in the B-horizon is caused by a preferential sorption of Ca on amorphous Fe-oxyhydroxides (0.25 M $NH_2OH{\cdot}HCl$-extractable), in which the Ca/Sr ratio was 364 (M. Land 1998, unpublished results). In the C-horizon the dissolved Ca/Sr ratio equals the solid Ca/Sr ratio. The dissolved Ca/Sr in the shallow groundwater is comparable with the ratio in the C-horizon soil water whereas the ratio in the deep groundwater is considerably higher, i.e., the ratio in the groundwater increases with depth. In the stream the Ca/Sr ratio is intermediate between the ratio in shallow and deep groundwater, respectively, but it is important to notice that surficial soil water may also have the potential to increase the ratio in the stream water.

5.2. $^{87}Sr/^{86}Sr$ ratios

^{87}Sr is a radiogenic isotope generated by emission of a negative β-particle from ^{87}Rb (e.g., Veizer, 1989). The $^{87}Sr/^{86}Sr$ ratio of a system is thus dependent on the initial ratio, the Rb content, and the age of the system. There are no Sr isotopic composition data for the soil and bedrock in the study area, but comparable lithologies in northern Sweden have been analysed for the $^{87}Sr/^{86}Sr$ ratio in other studies (e.g., Skiöld and Larsson, 1978; Skiöld, 1979; Skiöld, 1982; Öhlander and Billström 1989). By comparing the Rb content and age of these lithologies, the $^{87}Sr/^{86}Sr$ ratio of the parent soil material in the study area can be estimated to be 0.721–0.727. The exact value is not important in this context, but it illustrates that the dissolved $^{87}Sr/^{86}Sr$ ratio in the stream water is likely to be higher compared to the $^{87}Sr/^{86}Sr$ ratio in the bulk solid soil. This difference between the solid and dissolved $^{87}Sr/^{86}Sr$ ratio is due to the incongruent nature of the soil weathering. Biotite and K-feldspar possess a high Rb content and are thus usually relatively enriched in radiogenic ^{87}Sr. K-feldspar is rather resistant to weathering whereas biotite is more susceptible to weathering. If biotite dissolves at a higher rate than minerals containing less radiogenic Sr, an isotopic disequilibrium between the solid and dissolved phase can be generated. This Sr isotopic disequilibrium was also observed by Blum et al. (1993).

The $^{87}Sr/^{86}Sr$ ratio is obviously much higher in the deep groundwater compared to the soil water and shallow groundwater. Irrespective of the reason for this difference, the stream water appears to be a mixture of shallow groundwater and/or soil water (with lower $^{87}Sr/^{86}Sr$ ratios), and deep groundwater (with higher $^{87}Sr/^{86}Sr$ ratios). By plotting the $^{87}Sr/^{86}Sr$ ratio versus the reciprocal Sr concentration in a two component mixture, a straight mixing line is produced (e.g., Faure, 1986). $^{87}Sr/^{86}Sr$ is plotted vs 1/Sr in Fig. 6a. The stream water data fall substantially off a straight line between shallow groundwater/soil water and deep groundwater. The offset from the mixing line may be caused by the presence of a third component: meltwater or rain. Although the $^{87}Sr/^{86}Sr$ ratio in precipitation probably is far below the scale in Fig. 6, it is assumed in the following that the Sr isotopic composition in the stream water is not influenced by the pre-

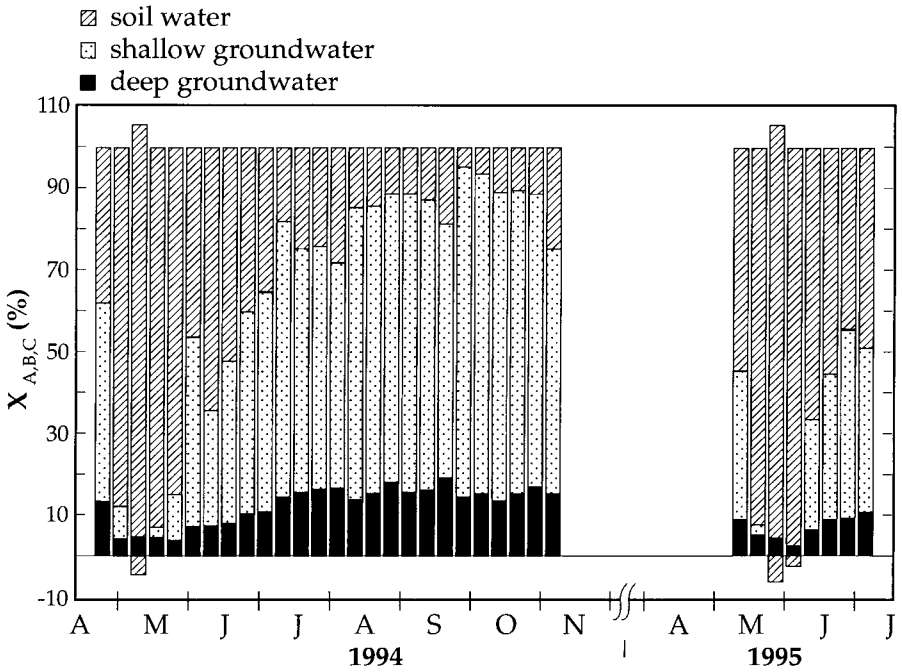

Fig. 7. Predicted fractions of soil water, shallow groundwater, and deep groundwater in the stream. At peak discharge during snowmelt the model overestimates the soil water component which is predicted to be >100%, whereas the shallow groundwater component is underestimated (<0%).

cipitation. This assumption is based on the very low Sr concentration in precipitation. In contrast, the Sr concentration is significantly diluted by the precipitation and 1/Sr is thus greatly increased. In Fig. 6b the $^{87}Sr/^{86}Sr$ ratio is plotted versus the Ca/Sr ratio. In this case the stream water data fall very close to a mixing line. This is most likely a consequence of the low concentrations of Ca and Sr in precipitation. The presence of precipitation does not influence the Ca/Sr ratio in the stream water, but merely dilutes these elements in approximately equal proportions. Fig. 6 illustrates the advantage of using element ratios rather than element concentrations for the mixing model in this case: dilute overland components may contribute substantially to the generation of stream water, but they do not interfere with the calculations of the relative contributions from the subsurface components (soil water, shallow groundwater and deep groundwater).

5.3. Application of Eq. (2)

In this section the stream water will be subdivided into the source components soil water (component A), shallow groundwater (component B), and deep groundwater (component C). This will be done by use of Ba/Sr and Ca/Sr ratios in these components. The dissolved Ca/Sr ratios in soil water from the Bs2- and C-horizons are very similar to each other. Soil water from the E- and Bs1-horizons is more problematic because the ratio in the E-horizon is higher and the ratio in the Bs1-horizon is lower than the ratio in the lower horizons. For simplicity, the concentrations of various elements in the soil water component are represented by an average of the concentrations in the different horizons. Starting with the Ca/Sr ratio, it is possible to determine the relative proportion of deep groundwater in the subsurface water discharge into the stream. When doing so, shallow groundwater and soil water are lumped together into a single component (component D). If the concentrations of Ca and Sr in component D are calculated as a mean of the concentrations in soil water and in shallow groundwater respectively, the relative proportion of deep groundwater in the subsurface water discharge into the stream water can be calculated according to Eq. (2) (note that similar Ca/Sr ratios in soil water and shallow groundwater is not a prerequisite). As a first approximation the soil water and shallow groundwater are given the same weight when calculating the Ca and Sr concentrations of component D.

By use of the Ba/Sr ratio, component D can be split into soil water (component A) and shallow groundwater (component B). In a 3 component mixture (m) with a known amount of the third component (X_k),

the fraction of the first component (X_i) can be calculated if Eq. (3) (derived in Appendix B) is applied,

$$\frac{X_i}{X_k} = \frac{\left(\frac{C^a}{C^b}\right)_m\left[C_j^b\left(1-\frac{1}{X_k}\right)-C_k^b\right]+C_j^a\left(\frac{1}{X_k}-1\right)+C_k^a}{\left(\frac{C^a}{C^b}\right)_m\left(C_i^b-C_j^b\right)+C_j^a-C_i^a} \quad (3)$$

where *i, j*, and *k* denote the components, a and b denote the elements, and *C* is concentration. When this is done the fraction of the second component (X_j) can be calculated by difference ($X_j = 1 - X_i - X_k$). If X_k is taken as the fraction of deep groundwater (X_C) calculated by Eq. (2), the fractions of soil water (X_A) and shallow groundwater (X_B) can be calculated by Eq. (3) and by difference, respectively. The next step is to go back and calculate a new Ca and Sr composition of component D using X_A and X_B as weights. It is then possible to recalculate X_C with Eq. (2) (using Ca/Sr ratios), and to recalculate X_A with Eq. (3) (using Ba/Sr ratios). Again, X_B is calculated by difference. When this iteration is repeated a number of times the fractions of components A, B, and C, respectively, will converge to stable values.

Fig. 7 shows the calculated fractions of soil water, shallow groundwater, and deep groundwater in the subsurface contribution to stream water. The amount of deep groundwater varies between approximately 5 and 20% with the highest values during base flow. It should be recognized, however, that even though the relative proportion of deep groundwater decreased during high discharge, the absolute discharge probably increased. During base flow the discharge of deep groundwater was approximately 3 l s^{-1}, whereas during snowmelt the deep groundwater discharge was about 35 l s^{-1} (assuming no contribution from precipitation).

Soil water dominates during snowmelt seasons, whereas during base flow it is the least important fraction. In fact, at peak discharge the model predicts that soil water accounts for slightly more than 100%. This overestimation could be an effect of the fact that precipitation and especially throughfall is less diluted with respect to Ba compared to Sr (if high Ba low Sr water reaches the stream via overland flow the model compensates for this by increasing the amount of soil water). However, the model does not make it possible to quantify the importance of the precipitation component in the stream water. Another factor that might contribute to the over-estimation of the soil water fraction is ion exchange and adsorption processes since the tracer elements most likely are non-conservative. However, if these reactions take place in the soil they should be accounted for by the model since the element ratios are known in both soil water and groundwater at all times. From Table 3 it can be seen that the Ba/Sr ratios in the E and Bs1 horizons start to increase when meltwater with low pH starts to percolate down the weathering profile in May. This result is what would be expected if Ba is adsorbed on clays and oxy-hydroxides to a larger extent than Sr. In October, when the soil has become much drier, the soil water seems to have re-equillibrated with the soil, resulting in lower dissolved Ba/Sr ratios. In the Bs1 horizon the dissolved Ca/Sr ratio decreased during percolation of meltwater. The trends for both the Ba/Sr and Ca/Sr ratios in the soil water are consistent with the findings of Nesbitt et al. (1980). On the other hand, if ion exchange reactions occur during mixing of the different water sources, or in the stream itself, the model will make false predictions. If, e.g., a significant amount of Ba is transported as adsorbed ions on particles to the stream, and upon arrival to the stream are released into solution, the fraction of soil water would be overestimated. Ingri and Widerlund (1994) showed that alkaline earths may be scavenged by suspended Fe and Mn oxy-hydroxides in river water. However, in the stream water in the present study only 6.8, 0.6 and 0.7% of the total Ba, Ca and Sr load, respectively, is transported in the suspended non-detrital (authigenic) matter (Land, 1998). This process would thus hava a limited effect on the dissolved Ba/Sr and Ca/Sr ratios in the stream water. In fact, adsorption processes would decrease the dissolved Ba/Sr since Ba is scavenged by the oxy-hydroxides to a larger extent than Sr, and consequently, the fraction of soil water in the stream water would be underestimated rather than overestimated by the model.

The fraction of shallow groundwater varies from <0 to 80% with the lowest values during peak discharge. As a consequence of the overestimation of the soil water component, the amount of shallow groundwater is underestimated during this period. At base flow shallow groundwater is the dominating fraction of the subsurface water discharge into the stream water.

5.4. Test of model validity

One way to check the model is to compare the measured $^{87}Sr/^{86}Sr$ ratios in the stream water with the $^{87}Sr/^{86}Sr$ ratios predicted by the model. The advantage of using isotopes in this context is that the element does not necessarily need to be conservative since the isotopic ratios are not influenced by processes such as adsorption and uptake by vegetation. During base flow in September the measured $^{87}Sr/^{86}Sr$ ratio in the stream water was 0.7381. On this occasion the calculated X_A, X_B, and X_C were 0.11, 0.75, and 0.14, re-

spectively. With Sr concentrations of 11.5, 20.0, and 52.2 μg l^{-1}, and with $^{87}Sr/^{86}Sr$ ratios of 0.7259, 0.7266, and 0.7605 in components A, B, and C, respectively, the model predicts a $^{87}Sr/^{86}Sr$ ratio of 0.7371. During snowmelt the model is somewhat less accurate. The measured and modelled $^{87}Sr/^{86}Sr$ ratios in the stream water were 0.7387 and 0.7347 at peak discharge 1994, 0.7388 and 0.7348 at early snowmelt 1995, and 0.7386 and 0.7342 just before peak discharge 1995, respectively. The modelled stream water data are plotted in Fig. 6b. There is a systematic underestimation of the $^{87}Sr/^{86}Sr$ ratio which may reflect the overestimation of the soil water fraction by the model. However, considering the large variation in $^{87}Sr/^{86}Sr$ ratios between the end members, the differences between measured and modelled $^{87}Sr/^{86}Sr$ ratios in the stream water are relatively small.

6. Conclusions

This study shows that element ratios can be useful as chemical tracers when the geochemistry of streams or rivers is to be interpreted. The developed model using Ba/Sr and Ca/Sr ratios as tracers is able to predict $^{87}Sr/^{86}Sr$ ratios in stream water that are well in accordance with measured values. It is shown that soil water can be a significant constituent of stream water during high discharge events such as spring flood during snowmelt. It is also shown that deep and relatively old groundwater contributes to stream water throughout the year. During base flow shallow groundwater is by far the most important stream water component.

Acknowledgements

This study was supported by grants from the Swedish Geological Survey, SGU. The chemical analyses were performed at SGAB Analys, Luleå. Support from the staff at this laboratory has been greatly appreciated. Sr-isotope analyses were performed at the Swedish Museum of Natural History. Discussions with Olov Marklund at the Division of Industrial Electronics, Luleå University of Technology, regarding the iterative model have been valuable. Milan Vnuk is greatly acknowledged for the help with the drawings. This paper was substantially improved by the thorough review from P. Shand and an anonymous reviewer.

Appendix A

Let $V_i + V_j = V_m$, where V denotes volume

$$C^a_m V_m = C^a_i V_i + C^a_j V_j \tag{A1}$$

$$C^b_m V_m = C^b_i V_i + C^b_j V_j \tag{A2}$$

Divide Eq. (A1) by Eq. (A2) and solve for V_i

$$V_i = V_j \frac{C^a_m C^b_j - C^b_m C^a_j}{C^b_m C^a_i - C^a_m C^b_i} \tag{A3}$$

Divide Eq. (A3) by $V_i + V_j$, let $X_i = V_i/(V_i + V_j)$ and rearrange

$$X_i = \frac{V_i}{V_i = V_j} = \frac{C^a_m C^b_j - C^b_m C^a_j}{C^b_m C^a_j \frac{V_i}{V_j} - C^a_m C^b_i \frac{V_i}{V_j} + C^b_m C^a_i - C^a_m C^b_i} \tag{A4}$$

Substitute V_i/V_j for $(C^a_m C^b_j - C^b_m C^a_j)/(C^b_m C^a_i - C^a_m C^b_i)$ and rearrange

$$X_i = \frac{1}{1 - \frac{\left(\frac{C^a}{C^b}\right)_m C^b_i - C^a_i}{\left(\frac{C^a}{C^b}\right)_m C^b_j - C^a_j}} \tag{A5}$$

Appendix B

Let $V_i + V_j + V_k = V_m = 1$, where V denotes volume.

$$C^a_m V_m = C^a_i V_i + C^a_j V_j + C^a_k V_k \tag{B1}$$

$$C^b_m V_m = C^b_i V_i + C^b_j V_j + C^b_k V_k \tag{B2}$$

Divide Eq. (B1) by Eq. (B2) and substitute V_j for $1 - V_i - V_k$. Rearrange and solve for V_i/V_k

$$\frac{V_i}{V_k} = \frac{C^b_m C^a_k - C^b_m C^a_j + C^a_m C^b_j - C^a_m C^b_k + C^b_m C^a_j \frac{1}{V_k} - C^a_m C^b_j \frac{1}{V_k}}{C^a_m C^b_i - C^a_m C^b_j + C^b_m C^a_j - C^b_m C^a_i} \tag{B3}$$

Let $X_i = V_i/(V_i + V_j + V_k) = V_i$, and $X_k = V_k/(V_i + V_j + V_k) = V_k$. Divide both numerator and denumerator by C^b_m and rearrange

$$\frac{X_i}{X_k} = \frac{\left(\frac{C^a}{C^b}\right)_m \left[C_j^b\left(1-\frac{1}{X_k}\right) - C_k^b\right] + C_j^a\left(\frac{1}{X_k}-1\right) + C_k^a}{\left(\frac{C^a}{C^b}\right)_m \left(C_i^b - C_j^b\right) + C_j^a - C_i^a} \quad \text{(B4)}$$

References

Åberg, G., Jacks, G., Hamilton, P.J., 1989. Weathering rates and $^{87}Sr/^{86}Sr$ ratios: an isotopic approach. J. Hydrol. 109, 65–78.

Andersson, P., Löfvendahl, R., Åberg, G., 1990. Major element chemistry, δ^2H, $\delta^{18}O$, and $^{87}Sr/^{86}Sr$ in a snow profile across central scandinavia. Atmospheric Environment 24A, 2601–2608.

Andersson, P., Ingri, J., Boström, K. 1991. Manganese in rain, throughfall and riverwater in north swedish coniferous forest. In Hydrogeochemistry of iron, manganese, and sulphur- and strontium isotopes in a coniferous catchment, central Sweden. Dissertation, Stockholm University.

Bazemore, D.E., Eshleman, K.N., Hollenbeck, K.J., 1994. The role of soil water in stormflow generation in a forested headwater catchment: synthesis of natural tracer and hydrometric evidence. J. Hydrol. 162, 47–75.

Beven, K.J., Germann, P., 1981. Water flow in soil macropores; I and II. J. Soil Sci. 32, 1–29.

Blum, J.D., Erel, Y., Brown, K., 1993. $^{87}Sr/^{86}Sr$ ratios of Sierra Nevada stream waters: implications for relative mineral weathering rates. Geochim. Cosmochim. Acta 57, 5019–5025.

Bullen, T., White, A., Blum, A., Harden, J., Schulz, M., 1997. Chemical weathering of a soil chronosequence on granitoid alluvium: II. Mineralogic and isotopic constraints on the behaviour of strontium. Geochim. Cosmochim. Acta 61, 291–306.

Eriksson, E., 1974. Vattnet -kemikaliebäraren. Forskning och Framsteg 5, 41–46 (in Swedish).

Faure, G., 1986. Principles of Isotope Geology, 2nd ed. Wiley, New York.

Faure, G., Powell, J.L., 1972. Strontium Isotope Geology. Springer, Berlin.

Granat, L., 1990. Luft- och nrderbördskemiska stationsnätet inom PMK, Swedish environmental protection agency, report 3942, (In Swedish).

Hooper, R.P., Christophersen, N., Peters, N.E., 1990. Modelling streamwater chemistry as a mixture of soilwater end-members — an application to the Panola Mountain catchment, Georgia, USA. J. Hydrol. 116, 321–343.

Horton, R.E., 1933. The role of infiltration in the hydrologic cycle. Eos Trans. AGU 14, 446–460.

Ingri, J., Widerlund, A., 1994. Uptake of alkali and alkaline earth elements on suspended iron and manganese in the Kalix River, northern Sweden. Geochim. Cosmochim. Acta 58, 5433–5442.

Ingri, J., Torsander, P., Andersson, P.S., Mörth, C-M., Kusakabe, M., 1997. Hydrogeochemistry of sulfur isotopes in the Kalix river catchment, northern Sweden. Appl. Geochem. 12, 483–496.

Ingri, J., Widerlund, A., Land, M. 1998. Dissolved major element ratios as tracers for hydrological compartments and flowpaths in the Kalix River catchment, northern Sweden. In (M. Land) Weathering of till in northern Sweden and its implications for the geochemistry of soil water, groundwater and stream water. Luleå University of Technology, Doctoral thesis.

Jacks, G., Åberg, G., Hamilton, P.J., 1989. Calcium budgets for catchments as interpreted by strontium isotpes. Nord. Hydrol. 20, 85–96.

Land, M. 1998. Weathering of till in northern Sweden and its implications for the geochemistry of soil water, stream water and groundwater. Luleå University of Technology. Doctoral thesis.

Land, M., Öhlander, B., 1997. Seasonal variations in the geochemistry of shallow groundwater hosted in granitic till. Chem. Geol. 143, 205–216.

Langmuir, C.H., Vocke, R.D., Hanson, G.N., Hart, S.R., 1978. A general mixing equation with applications to icelandic basalts. Earth Planet. Sci. Lett. 37, 380–392.

Li, X., 1985. The discriminant equation for a three-component mixing model of isotopes and trace elements and its application. Diqiu Huaxue = Geochimica 3, 250–254.

Lundqvist, J., 1986. Late Weichselian glaciation and deglaciation in Scandinavia. In: Sibrava, V., Bowen, D.Q., Richmond, G.M. (Eds.), Quaternary glaciations in the northern hemisphere, Quaternary Sci. Rev., 5, pp. 269–292.

Mason, B., Moore, C.B., 1982. Principles of geochemistry, 4th ed. Wiley, New York.

Maulé, C.P., Stein, J., 1990. Hydrologic flowpath definition and partitioning of spring meltwater. Water Resour. Res. 26, 2959–2970.

Mulder, J., Pijpers, M., Christophersen, N., 1991. Water flow paths and the spatial distribution of soils and exchangeable cations in an acid rain-impacted and a pristine catchment in Norway. Water Resour. Res. 27, 2919–2928.

Nakano, T., Tanaka, T., Tsujimura, M., Matsutani, J. 1993 Strontium isotopes in soil-plant-atmosphere continuum (SPAC). Tracers in Hydrology (Proceedings of the Yokohama symposium, July 1993). IAHS Publ. No. 215, 1993.

Négrel, P., Allègre, C.J., Dupré, B., Lewin, E., 1993. Erosion sources determined by inversion of major and trace element ratios and strontium isotopic ratios in river water: The Congo Basin case. Earth Planet Sci. Lett. 120, 59–76.

Nesbitt, H.W., Markovics, G., Price, R.C., 1980. Chemical processes affecting alkalis and alkaline earths during continental weathering. Geochim. Cosmochim. Acta 44, 1659–1666.

Norrström, A.C., Jacks, G., 1996. Water pathways and chemistry at the groundwater/surface water interface to Lake Skjervatjern, Norway. Water Resour. Res. 32, 2221–2229.

Öhlander, B., Billström, K., 1989 Regional implications of U-Pb zircon dating of two proterozoic granites associated with molybdenite mineralized aplites in northern Sweden, GFF 111 229–238.

Öhlander, B., Land, M., Ingri, J., Widerlund, A., 1996. Mobility of rare earth elements during weathering of till in northern Sweden. Appl. Geochem. 11, 93–99.

Pearce, A.J., Stewart, M.K., Sklash, M.G., 1986. Storm runoff generation in humid headwater catchments 1. Where

does the water come from? . Water Resour. Res. 22, 1263–1272.

Perel'man, A.I., 1977. Geochemistry of elements in the supergene zone. Keter, Jerusalem.

Pin, C., Bassin, C., 1992. Evaluation of a strontium-specific extraction chromatographic method for isotope analysis in geological materials. Anal. Chim. Acta 269, 249–255.

Puchelt, H., 1972. Barium. In: Wedepohl, K.H. (Ed.), Handbook of Geochemistry. Springer, Berlin, pp. 56D1–56D18.

Robson, A., Neal, C., 1990. Hydrograph separation using chemical techniques: an application to catchments in mid-Wales. J. Hydrol. 116, 345–363.

Rodhe, A., 1981. Spring flood. Meltwater or groundwater? . Nordic Hydrol. 12, 21–30.

Rose, S., 1996. Temporal environmental isotopic variation within the falling creek (Georgia) watershed; implications for contributions to streamflow. J. Hydrol. 174, 243–261.

Skiöld, T., Larsson, C., 1978. Age data on proterozoic granitoids from the Norvijaur area of northern Sweden. GFF 100, 171–176.

Skiöld, T., 1979. U-Pb zircon and Rb-Sr whole rock and mineral ages of proterozoic intrusives on mapsheet Lannavaara, northern Sweden. GFF 101, 131–137.

Skiöld, T., 1982. Radiometric ages of plutonic and hypabyssal rocks from the Vittangi-Karesuando area, northern Sweden. GFF 103, 317–329.

Sklash, M.G., Farvolden, R.N., 1979. The role of groundwater in storm runoff. J. Hydrol. 43, 45–65.

Smettem, K.R.J., 1984. Soil-water residence time and solute uptake 3. Mass transfer under simulated winter rainfall conditions in undisturbed soil cores. J. Hydrol. 67, 235–248.

SMHI 1996. Väder och vatten. En tidning från SMHI-Väderåret 1995. Norrköping: Swedish Meteorological and Hydrological Institute. (in Swedish).

Soil, Survey Staff, 1995. Keys to soil taxonomy, 5th ed. Edition, SSMS Technical Monograph No. 19. Pocahontas Press, Blacksburg, Virginia.

Stein, J., Prolux, S., Lévesque, D., 1994. Forest floor frost dynamics during spring snowmelt in a boreal forested basin. Water Resour. Res. 30, 995–1007.

Stewart, B.W., Capo, R.C., Chadwick, O.A., 1998. Quantitative strontium isotope models for weathering, pedogenesis and biogeochemical cycling. Geoderma 82, 173–195.

Stueber, A.M., 1978. Strontium. In: Wedepohl, K.H. (Ed.), Handbook of Geochemistry, vol. II-4. Springer, Berlin, pp. 38D1–38D17.

Veizer, J., 1989. Strontium isotopes in seawater through time. Ann. Rev. Earth Planet. Sci. 17, 141–167.

Wels, C., Cornett, R.J., Lazerte, B.D., 1991. Hydrograph separation: a comparison of geochemical and isotopic tracers. J. Hydrol. 122, 253–274.